PNAS RESEARCH ARTICLE | PHYSICS

Correlation of plastic events with local structure in jammed packings across spatial dimensions

Sean A. Ridout[a,1], Jason W. Rocks[a], and Andrea J. Liu[a,1]

Edited by Pablo Debenedetti, Princeton University, Princeton, NJ; received October 19, 2021; accepted March 10, 2022

In frictionless jammed packings, existing evidence suggests a picture in which localized physics dominates in low spatial dimensions, $d = 2, 3$, but quickly loses relevance as d rises, replaced by spatially extended mean-field behavior. For example, quasilocalized low-energy vibrational modes and low-coordination particles associated with deviation from mean-field behavior (rattlers and bucklers) all vanish rapidly with increasing d. These results suggest that localized rearrangements, which are associated with low-energy vibrational modes, correlated with local structure, and dominant in low dimensions, should give way in higher d to extended rearrangements uncorrelated with local structure. Here, we use machine learning to analyze simulations of jammed packings under athermal, quasistatic shear, identifying a local structural variable, softness, that correlates with rearrangements in dimensions $d = 2$ to $d = 5$. We find that softness—and even just the local coordination number Z—is essentially equally predictive of rearrangements in all d studied. This result provides direct evidence that local structure plays an important role in higher d, suggesting a modified picture for the dimensional cross-over to mean-field theory.

glasses | structure | machine learning | mean-field theory | plasticity

Significance

Mean-field theories, exact in the limit of infinite spatial dimensions, succeed in describing many features of glasses and amorphous solids in low dimensions, leading to considerable effort to understand how behavior evolves with dimension. Until now, all evidence has supported a picture in which "localized physics," responsible for deviations from mean-field behavior in low dimensions, fades away with rising dimension. Our work shows that rearrangements, in which particles change relative positions leading to fluid-like response, reveal a different picture of dimensional cross-over. We find that rearrangements, which are localized in two- and three-dimensional systems and correlated with local structure, remain just as correlated with local structure up to five dimensions, suggesting that local structure is important even in high dimensions.

Mean-field calculations have emerged as a promising first-principles approach to understanding glasses and amorphous solids. Although these calculations are only exact in the limit of infinite spatial dimension ($d = \infty$), they successfully capture many qualitative phenomena (1, 2) in $d = 2, 3$, including the time dependence of glassy relaxation, signatures of a Gardner transition to a marginal glass phase, and aging behavior within this phase. Furthermore, mean-field theory captures some aspects of jamming criticality in $d = 2, 3$ quantitatively, including critical exponents and the d dependence of the prefactors of scaling laws (1, 3).

Despite these successes, many questions remain regarding the cross-over from low-dimensional behavior to mean-field theory with increasing d. The existing literature collectively supports a dimensional cross-over picture in which localized effects thwart some mean-field predictions in low d but recede with increasing d, leading to smooth convergence to the mean-field limit (4–8). For example, near the zero-temperature ($T = 0$) jamming transition, rattlers and bucklers (particles with too few or just enough contacts to be locally stable) cause the scaling of the low tail of the contact force distribution to differ from the mean-field prediction, but these particles become exponentially rare with increasing d (4, 5).

An unexplored aspect of the dimensional convergence to mean-field behavior is the nature of rearrangement events. This aspect is key to glassy dynamics because such events, in which particles experience large, sudden displacements and change their relative positions, are the mechanism by which supercooled liquids relax. Particle rearrangements are also responsible for plasticity in athermal jammed packings under mechanical load, such as shear strain. In low d, rearrangements are localized, and local structure plays an important role (9–27). In particular, machine learning has identified a linear combination of local structural quantities named "softness," which is highly predictive of rearrangements and provides insight into the underlying physics (18, 28–38).

In particular, local structure is predictive of localized rearrangements in systems under athermal, quasistatic shear in $d = 2, 3$ (18, 28, 37). Indirect evidence supports the prevailing dimensional cross-over picture, suggesting that this low-dimensional localized physics should diminish with increasing d, which leads to a decreasing correlation between local structure and rearrangements as d rises. First, at $T = 0$ in low d, each localized rearrangement corresponds to a quasilocalized vibrational normal mode whose frequency vanishes; as d increases, however, quasilocalized low-frequency modes are increasingly outnumbered by extended ones (6, 7). Second, structure becomes more homogeneous in higher d. Rattlers and bucklers, associated with soft deformations and deviations from mean-field behavior, disappear as d rises, and the SD of the relative excess coordination, σ_Z/Z_c,

Author affiliations: [a]Department of Physics and Astronomy, University of Pennsylvania, Philadelphia, PA 19104

Author contributions: S.A.R., J.W.R., and A.J.L. designed research; S.A.R. and J.W.R. performed research; S.A.R. and J.W.R. contributed new reagents/analytic tools; S.A.R. and J.W.R. analyzed data; and S.A.R., J.W.R., and A.J.L. wrote the paper.

The authors declare no competing interest.

This article is a PNAS Direct Submission.

[1]To whom correspondence may be addressed. Email: ridout@sas.upenn.edu or ajliu@physics.upenn.edu.

This article contains supporting information online at https://www.pnas.org/lookup/suppl/doi:10.1073/pnas.2119006119/-/DCSupplemental.

Published April 11, 2022.

decays asymptotically as $1/\sqrt{d}$, suggesting that in high d, all particles have very similar local environments (5). Based on these observations and the existing dimensional cross-over picture, one would expect a cross-over in d from localized rearrangements strongly correlated with local structure to extended rearrangements that are necessarily much less correlated with local structure.*

Here, we test this hypothesis directly by quantifying the importance of local structure as a function of d via the prediction accuracy of machine-learned softness in athermal quasistatically sheared (AQS) jammed packings in dimensions $d = 2$ to $d = 5$. Although local structure is known to be predictive for AQS in low dimensions (18, 28), mean-field theory predicts plasticity with qualitative features matching low-d behavior (43, 44), making this a natural system to explore the dimensional cross-over to mean-field behavior. In contrast to the expectation that local structure only matters in low d, we find that softness is no less predictive of rearrangements as d rises. Moreover, softness increasingly coincides with the number of interacting neighbors or coordination number, Z, for each particle. Altogether, our results suggest a different picture of dimensional cross-over for plasticity, in which the distribution of Z plays an important role and a particle's coordination number remains a valuable indicator of mobility even in the mean-field limit.

Approach

We first prepare bidisperse jammed packings of Hertzian particles at many pressures. Each system is then sheared athermally and quasistatically by applying small strain steps and minimizing the energy at each step. While past work considered static packings in spatial dimensions up to $d = 10$ (5–7), here we focus on $d = 2$ to 5 due to the much larger computational cost of quasistatic shear trajectories.

Next, we seek to identify structures that correlate with local fluctuations in the displacement field according to the framework established in ref. 38. In this scheme, we quantify local structure by counting the number of contacts and gaps at each distance in a triangulation of the packing. To describe the dynamics, we follow what has become standard practice (11, 18, 45) and train to predict the first rearrangement in each avalanche, rather than seeking to describe entire avalanches (37, 46). To do this, we compute the lowest eigenvector of the dynamical matrix immediately before the stress drop. Using this eigenvector, we compute the quantity D^2_{min} for each particle, measuring its nonaffine displacement relative to its neighbors (45, 47) (a precise definition is given in *Materials and Methods*). Because the system is solid, a rearranging particle exerts a long-ranged strain field on the system, causing power law decay of D^2_{min} with distance. Following previous work, we define a quantity $\Delta^2_{\text{min}} = D^2_{\text{min}}/\langle D^2_{\text{min}}\rangle$, where the average is carried out over neighbors. Thus, Δ^2_{min} describes local fluctuations in D^2_{min}.

Finally, we use linear regression to find a linear combination of our structural descriptors S, which correlates with Δ^2_{min}. The correlation coefficient R^2 for this regression is not high, but our goal is only to predict the rearrangement itself, not the full D^2_{min} field; we have shown previously that S trained this way is just as predictive of rearrangements as previous classification-based approaches but requires fewer training examples because all particles are used in the training rather than only a small subset (38). Further details on our approach can be found in *Materials and Methods*.

*We note that this is not a general property of mean-field theories, which may contain localized or even extended excitations that are correlated with notions of (simple) local structure (39–42), but of the current understanding of high-d structural glasses and the particular mean-field theory that has been developed for them.

Results

If a system has an extensive field of structural defects, under athermal quasistatic shear only one is triggered at the beginning of the avalanche, while the vast majority does not rearrange. Thus, to evaluate the predictive power of S, we must check not whether every particle with high S moves but whether the particle at the center of each rearrangement (the particle with the maximum value of D^2_{min} in the critical mode) has a high S (18, 48). We calculate the average percentile rank of S for rearranging particles, C_S, as our measure of correlation between structure and dynamics. A value of $C = 1$ corresponds to perfect prediction, while $C = 0.5$ corresponds to random guessing. We find that C_S calculated from linear regression is just as high as for previous classification-based approaches (38).

This quantification of prediction accuracy is superior to comparing classification accuracies on a training set or regression accuracies because those numbers depend on the definition of the training set, even if the resulting softness S does not change. An alternative approach is to set a threshold on D^2_{min} so that particles above this threshold are "rearranging," and then, to ask which fraction of these particles has high softness (37, 49). However, this means of quantifying prediction accuracy is problematic for us because different threshold D^2_{min} values must be selected for different dimensions and pressures, making meaningful comparisons across d and P impossible. In thermal systems, the isoconfigurational ensemble may be used to average over noise, allowing for completely threshold-free measures of correlation between structure and dynamics (20, 27), but the facts that a rearrangement may localize at a single defect and that it is necessarily coupled to an elastic response, which dictates much of most particles' motion (38, 50), preclude such an approach for athermal quasistatic shear.

In Fig. 1*A*, we report C_S for packings in all d as a function of pressure P. The error bars show an estimate of the uncertainty in C due to sampling error (38). We find that C_S is high, ranging from 0.85 to 0.9, and does not depend strongly on either P or d within uncertainty.

Although Fig. 1 shows that the local structure predicts the maximum of D^2_{min} equally well in all dimensions studied, the linear regression coefficient R^2, shown in Fig. 1 *A*, *Inset*, decays dramatically between $d = 2$ and $d = 5$. Thus, in higher dimensions, fluctuations in D^2_{min} are more poorly correlated with local structure, but the little correlation that remains is enough to identify a structural variable that correlates strongly with the rearrangement itself, as evidenced by the continuing high value of C_S. In other words, while S loses correlation with Δ^2_{min} overall, it remains correlated with the extreme high tail of D^2_{min} corresponding to rearrangements. For us, training on Δ^2_{min} is only a means of finding a quantity (softness) that correlates strongly with rearrangements; the fact that C_S remains high in all d studied clearly demonstrates that structure is no less predictive in higher d. Note that C_S provides a lower bound on what can be achieved by machine learning methods.

Most of the predictive power of S comes from the number of contacts at distance $d_{i,(j,k)} = 1$ (i.e., the coordination number Z of each particle). For comparison, we demonstrate the predictive power of Z by computing the average percentile of $-Z$, which we denote as C_Z. In Fig. 1*B*, we report C_Z for the same set of particles used to measure C_S. Except at high pressures, we see that C_Z is comparable with C_S and roughly independent of d; in $4d$ and $5d$, they are equal within uncertainty (Fig. 1 *B*, *Inset*). Thus, Z contains most of the local structural information in S, and it contains more and more of the available information with increasing d.

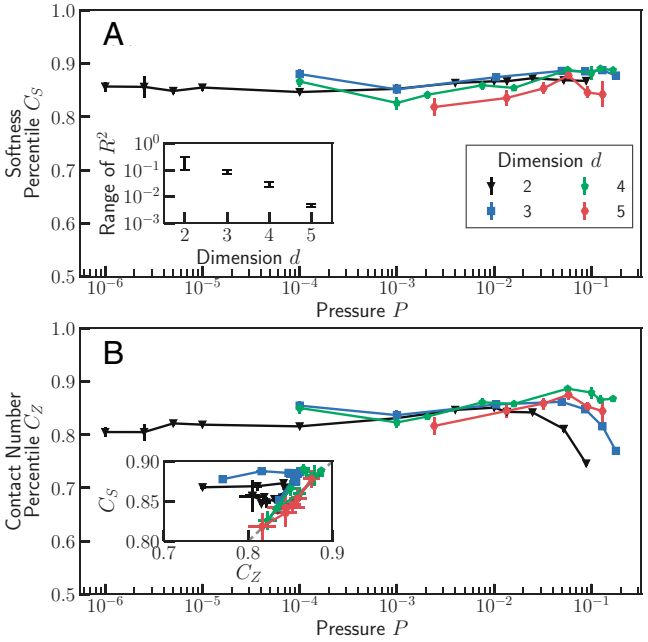

Fig. 1. The S percentile C_S (*A*) and the $-Z$ percentile C_Z (*B*) of the particle with the highest Δ^2_{min} in a plastic event as a function of dimension d and pressure P ($d = 2$, black triangles; $d = 3$, blue squares; $d = 4$, green pentagons; $d = 5$, red hexagons). Except for a weak decrease of C_Z at low P and a more dramatic decrease at very high P, predictiveness depends little on P and d within statistical uncertainties. Except at high pressure, Z performs almost as well as S. Error bars are uncertainty in the mean value. (*A*, *Inset*) R^2 for fitting of S to the local displacement fluctuations Δ^2_{min}. Error bars show the full range over all pressures; all data are shown in *SI Appendix* (*SI Appendix*, Fig. S4). Although the rearranging particle is predicted equally well in higher d, the correlation to the rescaled mobility field used to fit S is much worse in higher d. *B*, *Inset* shows that the correlation between C_S and C_Z is strong, except at high P, with them nearly coinciding in $d = 4, 5$.

Various length scales diverge at the jamming transition (51), including the scale of spatial correlations of Z (52) and the length scale below which linear elasticity fails (53). Diverging length scales are also observed in nonlinear response (e.g., in relaxation, finite strain rate, and granular experiments) (54–56). Thus, an approach based on a fixed number of local structural descriptors might be expected to perform more poorly as $P \to 0$ since the number of necessary descriptors should diverge. Surprisingly, neither C_S nor C_Z show a significant decrease with pressure. We further find that C_S shows no finite-size scaling at low pressures (*SI Appendix*, Fig. S5), further indicating that the slight decrease in accuracy at low pressures is unlikely to be due to a diverging length scale (57).

In retrospect, it is not surprising that S reduces simply to the coordination number Z at higher d. In infinite d, it suffices to truncate the virial expansion at second order (i.e., to only include the effects of the nearest interacting neighbors) (58). With increasing d, a particle's nearest neighbors are increasingly unlikely to also be neighbors of one another, so descriptors other than particle type, Z, and the number of nearest neighbor gaps should contain no information as $d \to \infty$.

What is surprising is that rearrangements still localize around low-Z particles as d increases, as shown by C_Z. Because the low-frequency vibrational modes at zero strain become extended in high d, one expects rearrangements to become less localized in higher dimensions, causing a decrease of C_Z (6, 7).

To determine the extent of localization of the initial rearrangement, we calculate the spatial correlations of D^2_{min} and Δ^2_{min}, along with those of S. At large distances, the D^2_{min} of each rearrangement displays power law decay, consistent with continuum elasticity, but at short distances, there is exponential decay in D^2_{min} correlations on the scale of the particle diameter (*SI Appendix*, Figs. S6–S11). This decay length gives a measure of the size of the rearrangement core, and we define it as the correlation length.

Fig. 2 shows the correlation lengths for D^2_{min}, Δ^2_{min}, and S as a function of P in all d. At low P in low d, the D^2_{min} correlation length grows but not as a power law and with no sign of diverging at unjamming. At high P and higher d, it appears to approach the S and Δ^2_{min} correlation lengths, which are approximately equal and pressure independent. The correlation lengths all decrease with increasing d, indicating that rearrangements become more localized spatially. In *SI Appendix*, we also provide the inverse participation ratio of the critical modes and compare them with previous reports at zero strain (*SI Appendix*, Fig. S1) (6, 7, 59). These results show that the delocalization of the lowest-frequency modes as $d \to \infty$ at zero strain does not necessarily imply delocalization of rearrangements at nonzero strain in higher d. Fewer and fewer quasilocalized modes exist (6, 7) with increasing d, but it appears that shearing picks one of the few remaining quasilocalized modes to go unstable, suggesting that the quasilocalized modes are more sensitive to shear strain than the extended disordered modes. This may not seem surprising when one considers that even in low dimensions, quasilocalized modes, which exist at arbitrarily low frequencies in the thermodynamic limit $N \to \infty$, are outnumbered by acoustic phonons but nevertheless, control plasticity. Our results suggest that the limits $\gamma \to \gamma_c$ and $d \to \infty$ do not commute; taking the former limit first yields localized rearrangements, while taking $d \to \infty$ first eliminates localized modes that could produce such rearrangements, leading to extended ones.

It is possible to construct disordered mean-field models with localized low-energy modes or modes that are either localized or extended that correlate with local structure (39–42). However, existing numerical work on our system (7) suggests convergence to the spectrum of the perceptron, with zero density of low-frequency localized modes, as $d \to \infty$ at $\gamma = 0$, N finite. Thus, mean-field models with a finite density of localized or quasilocalized low-frequency modes may not apply to these systems, where the density of states at the zero-strain ground state appears to converge to that of the perceptron, but nonetheless, a single localized mode dominates as the critical strain is approached, suggesting the existence of a subextensive but relevant set of localized modes.

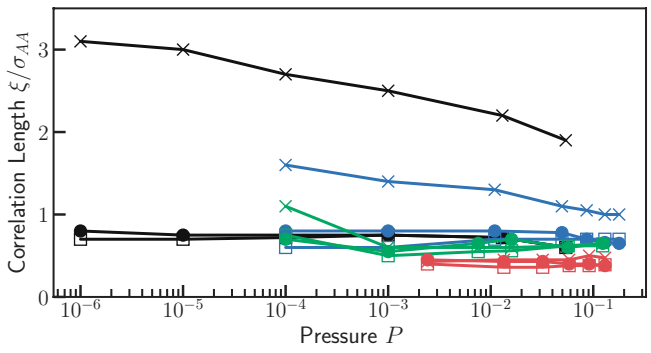

Fig. 2. Correlation lengths extracted from the fits to initial exponential decay of correlation functions as a function of pressure. In 2*d* and 3*d*, the D^2_{min} correlation length is much longer than that of S or Δ^2_{min}; in $d = 4, 5$, they appear almost equal. All correlation lengths appear to decrease with increasing spatial dimension. Black, 2*d*; blue, 3*d*; green, 4*d*; red, 5*d*. The x's indicate D^2_{min}, the open squares indicate Δ^2_{min}, and the circles indicate S.

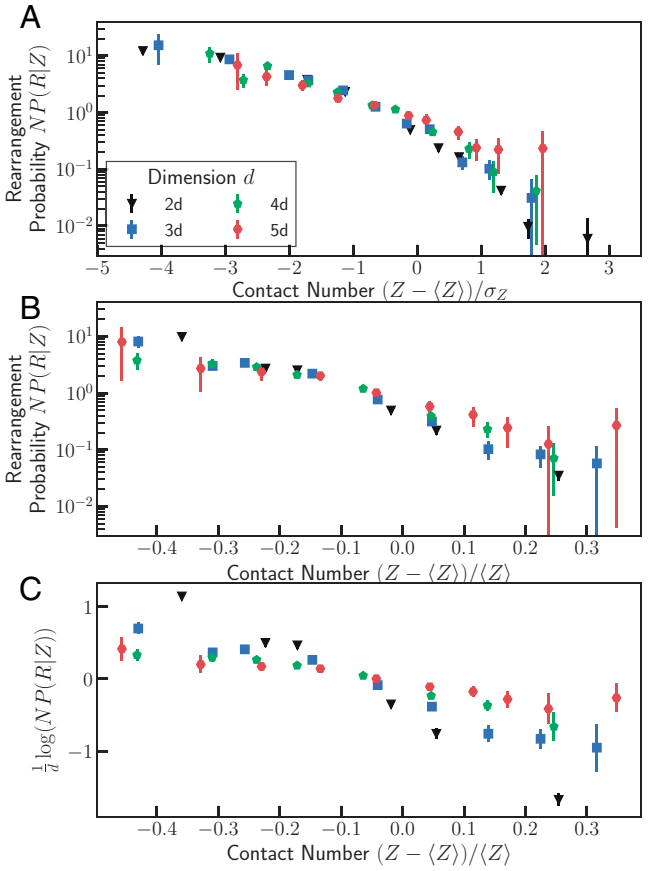

Fig. 3. Probability of rearranging for small particles as a function of $(Z - \langle Z \rangle)/\sigma_Z$ in varying spatial dimension as well as the statistics $\langle Z \rangle$ and σ_Z for small particles used to scale *Z*. (*A*) Probability of rearranging for small particles as a function of $(Z - \langle Z \rangle)/\sigma_Z$ in varying spatial dimension ($d = 2$, black triangles; $d = 3$, blue squares; $d = 4$, green pentagons; $d = 5$, red hexagons). After rescaling, data from all pressures before C_Z decreases are binned together. As *d* and *P* are varied, the dependence of the rearrangement probability on this rescaled *Z* is similar, indicating that particles with relatively low *Z* are always more likely to rearrange, even in higher *d* where they are not bucklers. Error bars indicate statistical uncertainty in the mean. (*B* and *C*) Alternate attempts at data collapse under different scenarios for the *d* dependence described in the text. These collapses are worse than that in *A*, and as shown in *SI Appendix*, Fig. S3, they become still worse when data from all pressures are plotted separately.

We also note recent work on the convergence to mean field in the (thermal) random Lorentz gas (60). This work found more complicated dimension dependence in dynamical properties due to an interplay between mean-field caging and percolation in finite-dimensional systems. In particular, however, they find that while mean-field theory correctly describes the dynamics at any finite time in large *d*, it fails to describe the percolation transition in any large finite dimension because the limit $t \to \infty$ fails to commute with that of $d \to \infty$, a scenario analogous to ours.

Fig. 2 shows that the correlation lengths of $\Delta^2_{\min}$ and S are the same, indicating that structural correlations set the size of $D^2_{\min}$ fluctuations (61). Earlier work concluded that the spatial correlations of $D^2_{\min}$ are the same as those of S (61); here, we find that spatial correlations of $D^2_{\min}$ are longer ranged in $d = 2, 3$. However, the systems studied in ref. 61 did not exhibit elastic correlations over as long a range as we find here due to friction or thermal fluctuations. The correlation lengths of $D^2_{\min}$ and $\Delta^2_{\min}$ in those systems are, therefore, likely to be far more similar.

It has previously been noted that "bucklers," particles with the minimum number of contacts for local stability, are associated with deviations from mean-field behavior and become vanishingly rare in higher-dimensional packings (5). This appears to contradict our finding that C_Z does not decrease with increasing *d*. To reconcile these results, we examine the probability that the rearrangement is located at a given small particle as a function of Z in each *d* in Fig. 3*A*. Since the pressure dependence is weak except at high *P*, we bin together data from all *P* before the drop in C_Z; full data are in *SI Appendix*, Fig. S3. Comparing systems at the same pressure is not necessarily meaningful since *P* has different units in different *d*. The prediction accuracy of local structure, however, appears to be roughly constant as long as the pressure is not extremely high, justifying the average over *P*.

The curves collapse within error bars when Z is standardized by subtracting its mean $\langle Z \rangle$ and dividing by its SD σ_Z. This collapse demonstrates that it is a particle's coordination number relative to the distribution that determines its propensity to rearrange, rather than solely its status as a buckler or a rattler. The lower the standardized Z is, the higher the probability is to rearrange. In the limit $d \to \infty$, the standardized Z of rattlers and bucklers approaches $-\infty$, and they are never observed. Most rearranging particles have a value of Z that lies low in the distribution, consistent with Fig. 1*B*. Indeed, our data suggest that it is particles with values of Z lying one to two SDs below the mean that are most likely to be the locus of a rearrangement in all *d*.

Fig. 3 *B* and *C* addresses two other possible asymptotic behaviors of $P(R|Z)$. Defining $x = 2Z/\langle Z \rangle \sim Z/d$, there are three different scenarios that could prevail in high *d*. 1) Our results favor the scenario summarized in Fig. 3*A*, where $P(R|Z) = f((Z - \langle Z \rangle)/\sigma_Z)$. Since the dynamics are a function of Z/σ_Z rather than $Z/\langle Z \rangle$, x is insufficient to describe the physics; $x^* \to 2$ as $d \to \infty$, but $2 - x^*$ goes to zero at the same rate as σ_x. So, rearranging particles are still atypical, and C_Z is constant. 2) One may have naïvely expected that only particles with extremely low $Z/\langle Z \rangle$, such as bucklers, act as structural defects. This scenario is made mathematically precise by assuming that $P(R|Z) = f(x)$. Since $\sigma_x \sim 1/\sqrt{d}$, the typical x^* for rearranging particles goes to one, and $C_Z \to \frac{1}{2}$ (no correlation) as $d \to \infty$. This scenario is consistent with the existing picture that localized physics becomes irrelevant in high dimensions. We do not, however, find a decrease in C_Z with spatial dimension, and Fig. 3*B* and especially *SI Appendix*, Fig. S3 show that the collapse of $P(R|Z)$ predicted by this scenario is not as good as the first. 3) It has been found in the past that the distribution of contacts in large *d* has a large-deviation form $P(Z) \sim e^{-dB(x)}$ (5). One might expect an analogous form $P(R|Z) \sim e^{-dA(x)}$, where $A(x) \sim x$ near the bulk of the distribution to reproduce the apparent exponential dependence of $P(R|Z)$. If $B(x)$ and $A(x)$ are expanded near the typical $x = 2$, one predicts $x^* = 2 - A'(2)/B''(2)$ (i.e., $1 < x^* < 2$); rearranging particles in large dimension are not necessarily bucklers but are still extremely atypical, and since $\sigma_x \to 0$ while $x^* - x$ is finite, $C_Z \to 1$ as $d \to \infty$. Thus, in this third scenario, the coordination Z predicts rearrangements perfectly in the mean-field limit. We do not see evidence for this increase in accuracy with *d*, and Fig. 3*C* and *SI Appendix*, Fig. S3 show again that this form does not collapse the data as well as scenario 1.

In *SI Appendix*, Fig. S2, we show the dependence of $\langle Z \rangle$ and σ_Z on *P* and *d*. We see that $\langle Z \rangle(P \to 0) \sim d$ as expected. However, we find that in $d = 2 - 5$, $\sigma_Z(P \to 0)$ seems to be crossing over from scaling like *d* to the expected $\sqrt{d}$ scaling (5). There is thus a small caveat to our results that at least σ_Z has not yet reached its asymptotic scaling in $d = 5$. Nonetheless, the collapse in Fig. 3*A* and *SI Appendix*, Fig. S3 suggests that $P(R|Z)$ has converged to a form that implies that Z remains an accurate predictor in all *d*.

Discussion

Our results suggest a revision of the picture relating low-dimensional to mean-field behavior, at least in jammed packings. In contrast to expectation, local structure remains important in determining particle rearrangements for all d. In high d, the contact number Z for each particle becomes a good structural predictor of rearrangements, implying that rearrangements are controlled only by nearest neighbors that interact directly with a particle. Although the contact number distribution narrows relative to the mean contact number $\langle Z \rangle \sim d$, the SD diverges, scaling as $\sigma_Z \sim \sqrt{d}$ (5). Thus, different particles can still have different Z in high dimensions as $d \to \infty$, and low Z particles may still have a higher propensity to rearrange. It should be possible to capture such behavior in a mean-field description of structural glasses. For example, recent work has shown how mean-field spin glass models can have low-energy modes that localize on sites with a low local magnetic field (which acts as a heterogeneous structural variable) (41, 42). In those models, this correlation is proven by studying the low-energy vibrational modes; as discussed above, however, our picture suggests that such a computation for structural glasses must be carried out at nonzero applied strain before the limit $d \to \infty$ is taken. Another possible route suggested by our work is a computation of $P(R|Z)$ in mean field [e.g., by computing $P(Z|R)$ for some suitable identification of R with mobility and then using Bayes' theorem].

Previous work has assumed or supported a scenario, such as scenarios 2 and 5–7, but our results do not. Rather, they suggest the possibilities of scenarios 1 and 3. Scenario 1, in which rearrangements localize at particles of low Z and C_Z is independent of d, is most consistent with our data. Either scenario 1 or 3 would reconcile the softness picture of dynamical behavior in low d with mean-field theory; in both cases, a particle's coordination number is the local structural variable that controls the particle's propensity to rearrange in high dimensions.

Materials and Methods

Simulations. We prepare bidisperse jammed packings of Hertzian particles at many pressures in each spatial dimension: that is, with the pair potential

$$U = \frac{\epsilon}{2} \sum \left(1 - \frac{r_{ij}}{\sigma_i + \sigma_j}\right)^{5/2} \theta(\sigma_i + \sigma_j - r_{ij}), \qquad [1]$$

with σ_i the radius of particle i and $\theta(x)$ the step function. The two particle radii are σ and 1.4σ.

We study $N = 4,096$ particles in $2d$, $N = 8,192$ in $3d$ and $4d$, and $N = 16,384$ in $5d$. Initially, particles are assigned random positions ($T = \infty$) before quenching to an energy minimum, producing a force-balanced, zero-temperature state. The system is sheared quasistatically by applying small strain steps ($\delta\gamma = 10^{-4}$) and reminimizing the energy E with respect to $\{x_i\}$ at each step. Commonly, an affine deformation field is used as the "guess" for the new positions before minimization at each step; during the linear elastic branches, we speed up the simulation by using the nonaffine displacements from the previous strain step as the initial guess.

When the pressure P is large, it is insensitive to shear ($\frac{1}{P}\frac{\partial P}{\partial \gamma} \approx 0$), allowing us to hold the volume V fixed. However, when P is small, it fluctuates with shear, so we fix P by minimizing the enthalpy, $H = E + PV$, with respect to both $\{x_i\}$ and V (62). When a plastic event is detected in the form of a drop in shear stress, the resulting state is discarded, and the stress drop is approached with a shear step $\delta\gamma/2$ (63, 64). We repeat this procedure until the stress drop is approached with a shear step of $\delta\gamma = 10^{-12}$, and the main obstruction to realizing true quasistatic shear is the force tolerance in the energy minimization algorithm (65, 66).

Structural Descriptors. We quantify local structure by finding a combination of local structural descriptors that captures each particle's propensity to rearrange. In previous studies, populations of rearranging and nonrearranging particles were identified from a collection of configurations and used to train a classifier to sort particles into these two groups (28). Here, we use linear regression to identify structures that correlate with local fluctuations in the displacement field (38). This method needs far less data to construct a good training set as it can use all particles rather than a small subset.

We describe each particle's structure by counting the number of contacts and gaps at each distance in a triangulation of the packing (38). Once the Delaunay triangulation of the packing is constructed, each particle j in the triangulation is assigned a discrete distance d_{ij} to particle i such that $d_{ii} = 0$, $d_{ij} = 1$ for neighbors, $d_{ij} = 2$ for particles sharing a neighbor, etc. Each edge (j, k) in the triangulation is either a contact between particles or a gap and is assigned a distance from particle i, $d_{i,(j,k)} = d_{ij} + d_{jk}$. The numbers of gaps and contacts at each distance up to $d_{i,(j,k)} = 8$, together with the particle radius, form a set of 17 descriptors that we use to encode the local structural environment around each particle.

Identifying the Initial Rearrangement and Computing D^2_{min}. One complication is that quasistatically sheared packings exhibit avalanches in which one localized rearrangement triggers a second and so on at each stress drop (46). To focus on localized rearrangements rather than avalanches, we follow what has become standard practice (11, 18, 45), training to predict the first rearrangement in each avalanche by computing the lowest eigenvector of the dynamical matrix $H_{ij} = \partial^2 U/\partial x_i \partial x_j$ immediately before the stress drop. This eigenvector is the normal mode whose frequency vanishes at the onset of the rearrangement, signaling the rearrangement. Using this eigenvector, we compute the quantity D^2_{min} for each particle, measuring its nonaffine displacement relative to its neighbors (45, 47).

We define D^2_{min} using the two nearest neighbor shells: that is, for a displacement eigenvector u,

$$D^2_{\text{min},i} = \frac{1}{N_i} \sum_{j, d_{ij} \leq 2} \left(\mathbf{u}_i - \mathbf{u}_j - \Lambda_i \mathbf{r}_{ij}\right)^2, \qquad [2]$$

where $N_i = \sum_{j,d_{ij}\leq 2} 1$ and Λ_i is chosen to minimize D^2_{min}.

Definition of Δ^2_{min} and Linear Regression. Because the system is solid, a rearranging particle exerts a long-ranged strain field on the system, causing power law decay of D^2_{min} with distance. A particle near the rearrangement shifts more than one far from it, regardless of their respective structural environments. To cancel this effect, we rescale D^2_{min} for each particle by dividing by the average D^2_{min} of its neighbors (38); we denote this quantity as Δ^2_{min}. Thus,

$$\Delta^2_{\text{min},i} = \frac{N_i D^2_{\text{min},i}}{\sum_{j,d_{ij}\leq 2} D^2_{\text{min},j}}. \qquad [3]$$

We find that Δ^2_{min} correlates far better with local structure than D^2_{min} (38).

Next, we perform linear regression to identify a linear combination of our structural descriptors, the softness S, which best correlates with Δ^2_{min}. Although the correlation coefficient R^2 is not high, our training variable Δ^2_{min} does not directly correspond to rearranging and non-rearranging particles, so R^2 does not quantify the prediction of rearrangements.

Data Availability. Raw data used to make plots and other data are published on Figshare (https://doi.org/10.6084/m9.figshare.19352048). Code is published on GitHub (https://github.com/saridout/structure_dynamics_across_dimensions_code).

ACKNOWLEDGMENTS. We thank Ge Zhang, Sam Schoenholz, Robert Ivancic, François Landes, Eric Corwin, and Francesco Zamponi for helpful discussions and Carl Goodrich, Sam Schoenholz, and Daniel Sussman for providing useful code. We thank the anonymous reviewers. This research was supported by a Natural Sciences and Engineering Research Council of Canada postgraduate scholarship doctoral award (to S.A.R.); Simons Foundation for the Collaboration Cracking the Glass Problem Award 454945 (to S.A.R., J.W.R., and A.J.L.) and Investigator Award 327939 (to A.J.L.); and US Department of Energy, Office of Basic Energy Sciences, Division of Materials Sciences and Engineering Award DE-FG02-05ER46199 (to J.W.R.).

1. P. Charbonneau, J. Kurchan, G. Parisi, P. Urbani, F. Zamponi, Glass and jamming transitions: From exact results to finite-dimensional descriptions. *Annu. Rev. Condens. Matter Phys.* **8**, 265–288 (2017).
2. L. Berthier *et al.*, Gardner physics in amorphous solids and beyond. *J. Chem. Phys.* **151**, 010901 (2019).
3. J. D. Sartor, S. A. Ridout, E. I. Corwin, Mean-field predictions of scaling prefactors match low-dimensional jammed packings. *Phys. Rev. Lett.* **126**, 048001 (2021).
4. P. Charbonneau, E. I. Corwin, G. Parisi, F. Zamponi, Universal microstructure and mechanical stability of jammed packings. *Phys. Rev. Lett.* **109**, 205501 (2012).
5. P. Charbonneau, E. I. Corwin, G. Parisi, F. Zamponi, Jamming criticality revealed by removing localized buckling excitations. *Phys. Rev. Lett.* **114**, 125504 (2015).
6. P. Charbonneau, E. I. Corwin, G. Parisi, A. Poncet, F. Zamponi, Universal non-debye scaling in the density of states of amorphous solids. *Phys. Rev. Lett.* **117**, 045503 (2016).
7. M. Shimada, H. Mizuno, L. Berthier, A. Ikeda, Low-frequency vibrations of jammed packings in large spatial dimensions. *Phys. Rev. E* **101**, 052906 (2020).
8. L. Berthier, P. Charbonneau, J. Kundu, Finite dimensional vestige of spinodal criticality above the dynamical glass transition. *Phys. Rev. Lett.* **125**, 108001 (2020).
9. A. Widmer-Cooper, H. Perry, P. Harrowell, D. R. Reichman, Irreversible reorganization in a supercooled liquid originates from localized soft modes. *Nat. Phys.* **4**, 711–715 (2008).
10. A. Widmer-Cooper, H. Perry, P. Harrowell, D. R. Reichman, Localized soft modes and the supercooled liquid's irreversible passage through its configuration space. *J. Chem. Phys.* **131**, 194508 (2009).
11. M. L. Manning, A. J. Liu, Vibrational modes identify soft spots in a sheared disordered packing. *Phys. Rev. Lett.* **107**, 108302 (2011).
12. S. S. Schoenholz, A. J. Liu, R. A. Riggleman, J. Rottler, Understanding plastic deformation in thermal glasses from single-soft-spot dynamics. *Phys. Rev. X* **4**, 031014 (2014).
13. M. Tsamados, A. Tanguy, C. Goldenberg, J. L. Barrat, Local elasticity map and plasticity in a model Lennard-Jones glass. *Phys. Rev. E Stat. Nonlin. Soft Matter Phys.* **80**, 026112 (2009).
14. L. Gartner, E. Lerner, Nonlinear plastic modes in disordered solids. *Phys. Rev. E* **93**, 011001 (2016).
15. J. Zylberg, E. Lerner, Y. Bar-Sinai, E. Bouchbinder, Local thermal energy as a structural indicator in glasses. *Proc. Natl. Acad. Sci. U.S.A.* **114**, 7289–7294 (2017).
16. A. Malins, J. Eggers, C. P. Royall, S. R. Williams, H. Tanaka, Identification of long-lived clusters and their link to slow dynamics in a model glass former. *J. Chem. Phys.* **138**, A535 (2013).
17. H. Tong, H. Tanaka, Revealing hidden structural order controlling both fast and slow glassy dynamics in supercooled liquids. *Phys. Rev. X* **8**, 011041 (2018).
18. D. Richard *et al.*, Predicting plasticity in disordered solids from structural indicators. *Phys. Rev. Materials* **4**, 113609 (2020).
19. S. Marín-Aguilar, H. H. Wensink, G. Foffi, F. Smallenburg, Tetrahedrality dictates dynamics in hard sphere mixtures. *Phys. Rev. Lett.* **124**, 208005 (2020).
20. V. Bapst *et al.*, Unveiling the predictive power of static structure in glassy systems. *Nat. Phys.* **16**, 448–454 (2020).
21. E. Boattini *et al.*, Autonomously revealing hidden local structures in supercooled liquids. *Nat. Commun.* **11**, 5479 (2020).
22. L. Viitanen, J. R. M. Intyre, J. Koivisto, A. Puisto, M. Alava, Machine learning and predicting the time dependent dynamics of local yielding in dry foams. *Phys. Rev. Res.* **2**, 023338 (2020).
23. E. Boattini, F. Smallenburg, L. Filion, Averaging local structure to predict the dynamic propensity in supercooled liquids. *Phys. Rev. Lett.* **127**, 088007 (2021).
24. J. Paret, R. L. Jack, D. Coslovich, Assessing the structural heterogeneity of supercooled liquids through community inference. *J. Chem. Phys.* **152**, 144502 (2020).
25. M. Lerbinger, A. Barbot, D. Vandembroucq, S. Patinet, *On the relevance of shear transformations in the relaxation of supercooled liquids.* arXiv [Preprint] (2021). https://arxiv.org/abs/2109.12639 (Accessed 1 February 2022).
26. S. Mitra, S. Marin-Aguilar, S. Sastry, F. Smallenburg, G. Foffi, *Correlation between plastic rearrangements and local structure in a cyclically driven glass.* arXiv [Preprint] (2021). https://arxiv.org/abs/2111.04116?context=cond-mat (Accessed 1 February 2022).
27. R. Díaz Hernández Rojas, G. Parisi, F. Ricci-Tersenghi, Inferring the particle-wise dynamics of amorphous solids from the local structure at the jamming point. *Soft Matter* **17**, 1056–1083 (2021).
28. E. D. Cubuk *et al.*, Identifying structural flow defects in disordered solids using machine-learning methods. *Phys. Rev. Lett.* **114**, 108001 (2015).
29. S. S. Schoenholz, E. D. Cubuk, D. M. Sussman, E. Kaxiras, A. J. Liu, A structural approach to relaxation in glassy liquids. *Nat. Phys.* **12**, 469–471 (2016).
30. D. M. Sussman, S. S. Schoenholz, E. D. Cubuk, A. J. Liu, Disconnecting structure and dynamics in glassy thin films. *Proc. Natl. Acad. Sci. U.S.A.* **114**, 10601–10605 (2017).
31. T. A. Sharp *et al.*, Machine learning determination of atomic dynamics at grain boundaries. *Proc. Natl. Acad. Sci. U.S.A.* **115**, 10943–10947 (2018).
32. M. Harrington, D. J. Durian, Anisotropic particles strengthen granular pillars under compression. *Phys. Rev. E* **97**, 012904 (2018).
33. X. Ma *et al.*, Heterogeneous activation, local structure, and softness in supercooled colloidal liquids. *Phys. Rev. Lett.* **122**, 028001 (2019).
34. F. P. Landes, G. Biroli, O. Dauchot, A. J. Liu, D. R. Reichman, Attractive versus truncated repulsive supercooled liquids: The dynamics is encoded in the pair correlation function. *Phys. Rev. E* **101**, 010602 (2020).
35. E. D. Cubuk, A. J. Liu, E. Kaxiras, S. S. Schoenholz, *Unifying framework for strong and fragile liquids via machine learning: A study of liquid silica*. arXiv [Preprint] (2020). https://arxiv.org/abs/2008.09681 (Accessed 1 October 2021).
36. I. Tah, T. A. Sharp, A. J. Liu, D. M. Sussman, Quantifying the link between local structure and cellular rearrangements using information in models of biological tissues. *Soft Matter* **17**, 10242–10253 (2021).
37. G. Zhang, S. Ridout, A. J. Liu, Interplay of rearrangements, strain, and local structure during avalanche propagation. arXiv [Preprint] (2020). https://arxiv.org/abs/2009.11414 (Accessed 1 October 2021).
38. J. W. Rocks, S. A. Ridout, A. J. Liu, Learning-based approach to plasticity in athermal sheared amorphous packings: Improving softness. *APL Materials* **9**, 021107 (2021).
39. E. Bouchbinder, E. Lerner, C. Rainone, P. Urbani, F. Zamponi, Low-frequency vibrational spectrum of mean-field disordered systems. *Phys. Rev. B* **103**, 174202 (2021).
40. G. Folena, P. Urbani, Marginal stability of local energy minima in soft anharmonic mean field spin glasses. arXiv [Preprint] (2021). https://arxiv.org/abs/2106.16221 (Accessed 1 February 2022).
41. S. Franz, F. Nicoletti, G. Parisi, F. Ricci-Tersenghi, Delocalization transition in low energy excitation modes of vector spin glasses. *SciPost Phys.* **12**, 016 (2022).
42. S. Franz, F. Nicoletti, F. Ricci-Tersenghi, Low energy excitations of mean-field glasses. arXiv [Preprint] (2022). https://arxiv.org/abs/2201.01607 (Accessed 1 February 2022).
43. S. Franz, S. Spigler, Mean-field avalanches in jammed spheres. *Phys. Rev. E* **95**, 022139 (2017).
44. P. K. Morse *et al.*, A direct link between active matter and sheared granular systems. *Proc. Natl. Acad. Sci. U.S.A.* **118**, e2019909118 (2021).
45. C. E. Maloney, A. Lemaître, Amorphous systems in athermal, quasistatic shear. *Phys. Rev. E Stat. Nonlin. Soft Matter Phys.* **74**, 016118 (2006).
46. S. Tewari *et al.*, Statistics of shear-induced rearrangements in a two-dimensional model foam. *Phys. Rev. E Stat. Phys. Plasmas Fluids Relat. Interdiscip. Topics* **60**, 4385–4396 (1999).
47. M. L. Falk, J. S. Langer, Dynamics of viscoplastic deformation in amorphous solids M. *Phys. Rev. E Stat. Phys. Plasmas Fluids Relat. Interdiscip. Topics* **57**, 14 (1998).
48. S. Patinet, D. Vandembroucq, M. L. Falk, Connecting local yield stresses with plastic activity in amorphous solids. *Phys. Rev. Lett.* **117**, 045501 (2016).
49. E. D. Cubuk, S. S. Schoenholz, E. Kaxiras, A. J. Liu, Structural properties of defects in glassy liquids. *J. Phys. Chem. B* **120**, 6139–6146 (2016).
50. A. Moriel, Y. Lubomirsky, E. Lerner, E. Bouchbinder, Extracting the properties of quasilocalized modes in computer glasses: Long-range continuum fields, contour integrals, and boundary effects. *Phys. Rev. E* **102**, 033008 (2020).
51. A. J. Liu, S. R. Nagel, The jamming transition and the marginally jammed solid. *Annu. Rev. Condens. Matter Phys.* **1**, 347–369 (2010).
52. D. Hexner, A. J. Liu, S. R. Nagel, Two diverging length scales in the structure of jammed packings. *Phys. Rev. Lett.* **121**, 115501 (2018).
53. E. Lerner, E. DeGiuli, G. Düring, M. Wyart, Breakdown of continuum elasticity in amorphous solids. *Soft Matter* **10**, 5085–5092 (2014).
54. Y. Nishikawa, A. Ikeda, L. Berthier, Relaxation dynamics of non-Brownian spheres below jamming. *J. Stat. Phys.* **182**, 37 (2021).
55. P. Olsson, S. Teitel, Dynamic length scales in athermal, shear-driven jamming of frictionless disks in two dimensions. *Phys. Rev. E* **102**, 042906 (2020).
56. A. S. Keys, A. R. Abate, S. C. Glotzer, D. J. Durian, Measurement of growing dynamical length scales and prediction of the jamming transition in a granular material. *Nat. Phys.* **3**, 260–264 (2007).
57. C. P. Goodrich *et al.*, Jamming in finite systems: Stability, anisotropy, fluctuations, and scaling. *Phys. Rev. E Stat. Nonlin. Soft Matter Phys.* **90**, 022138 (2014).
58. G. Parisi, P. Urbani, F. Zamponi, *Theory of Simple Glasses: Exact Solutions in Infinite Dimensions* (Cambridge University Press, New York, NY, 2020).
59. M. Shimada, H. Mizuno, M. Wyart, A. Ikeda, Spatial structure of quasilocalized vibrations in nearly jammed amorphous solids. *Phys. Rev. E* **98**, 060901 (2018).
60. G. Biroli *et al.*, Interplay between percolation and glassiness in the random Lorentz gas. *Phys. Rev. E* **103**, L030104 (2021).
61. E. D. Cubuk *et al.*, Structure-property relationships from universal signatures of plasticity in disordered solids. *Science* **358**, 1033–1037 (2017).
62. S. Dagois-Bohy, B. P. Tighe, J. Simon, S. Henkes, M. van Hecke, Soft-sphere packings at finite pressure but unstable to shear. *Phys. Rev. Lett.* **109**, 095703 (2012).
63. M. S. van Deen *et al.*, Contact changes near jamming. *Phys. Rev. E Stat. Nonlin. Soft Matter Phys.* **90**, 020202 (2014).
64. P. Morse, S. Wijtmans, M. van Deen, M. van Hecke, M. L. Manning, Differences in plasticity between hard and soft spheres. *Phys. Rev. Res.* **2**, 023179 (2020).
65. E. Lerner, I. Procaccia, Locality and nonlocality in elastoplastic responses of amorphous solids. *Phys. Rev. E Stat. Nonlin. Soft Matter Phys.* **79**, 066109 (2009).
66. N. Xu, A. J. Liu, S. R. Nagel, Instabilities of jammed packings of frictionless spheres under load. *Phys. Rev. Lett.* **119**, 215502 (2017).